

UC Berkeley

UC Berkeley Previously Published Works

Title

Nucleon-level Effective Theory of $\mu \rightarrow e$ Conversion

Permalink

<https://escholarship.org/uc/item/9tn1d75f>

Author

Rule, Evan

Publication Date

2024-02-06

DOI

10.22323/1.413.0099

Copyright Information

This work is made available under the terms of a Creative Commons Attribution-NoDerivatives License, available at <https://creativecommons.org/licenses/by-nd/4.0/>

Peer reviewed

Nucleon-level Effective Theory of $\mu \rightarrow e$ Conversion

Evan Rule*

Department of Physics, University of California, Berkeley, CA 94720, USA

E-mail: erule@berkeley.edu

The Mu2e and COMET $\mu \rightarrow e$ collaborations plan to advance branching ratio sensitivities by four orders of magnitude, further constraining new sources of charged lepton flavor violation (CLFV). We formulate a non-relativistic nucleon-level effective theory for this process, in order to clarify what can and cannot be learned about CLFV operator coefficients from elastic $\mu \rightarrow e$ conversion. Utilizing state-of-the-art shell model wave functions, we derive bounds on operator coefficients from existing $\mu \rightarrow e$ conversion results, and estimate the improvement in these bounds that will be possible if Mu2e and COMET reach their design goals. In the conversion process, we employ a treatment of the lepton Coulomb physics that is very accurate, yet yields transparent results and preserves connections to standard-model processes like β decay and μ capture. The formulation provides a bridge between the nuclear physics needed in form factor evaluations and the particle physics needed to relate low-energy constraints from $\mu \rightarrow e$ conversion to UV sources of CLFV.

The 10th International Workshop on Chiral Dynamics - CD2021

15-19 November 2021

Online

*Speaker

Work done in collaboration with Wick C. Haxton, Kenneth McElvain and Michael J. Ramsey-Musolf, as reported in [1, 2].

1. Introduction

Experimental searches for processes which violate charged lepton flavor conservation are among the most sensitive probes of beyond Standard Model (BSM) physics. In this work, we focus on $\mu \rightarrow e$ conversion, the process in which a muon captured into the Coulomb field of an atomic nucleus converts into a mono-energetic outgoing electron. The relevant experimental quantity is the branching ratio

$$B(\mu^- + (A, Z) \rightarrow e^- + (A, Z)) \equiv \frac{\omega(\mu^- + (A, Z) \rightarrow e^- + (A, Z))}{\omega(\mu^- + (A, Z) \rightarrow \nu_\mu + A(Z - 1, N + 1))}, \quad (1)$$

where the denominator is the rate for standard muon capture. Depending on the nature of the underlying CLFV operators, the current upper limit $B(\mu \rightarrow e) < 7 \times 10^{-13}$ [3] constrains BSM physics up to energy scales $\sim 10^3$ TeV. The next generation experiments, Mu2e [4, 5] at Fermilab and the COherent Muon to Electron Transition (COMET) experiment [6] at Japan Proton Research Complex (J-PARC), aim to improve upon the existing branching ratio limit by as much as four orders of magnitude, potentially probing as high as 10^4 TeV. Both experiments have chosen ^{27}Al as the nuclear target, but an ensemble of measurements on various nuclear targets is a high priority beyond the initial experimental runs.

The remarkable sensitivities achieved in $\mu \rightarrow e$ conversion experiments are made possible by the kinematics: assuming that the nucleus remains in the ground state, electrons emitted through the CLFV conversion process will have an energy at the very endpoint of the spectrum of background electrons originating from standard model $\mu \rightarrow e + 2\nu$ decays. Close to the endpoint energy, the standard model muon decays are suppressed by a factor $(E_{\text{endpoint}} - E)^5$ leading to extremely low backgrounds in the region of interest. However, the restriction of the nucleus to the ground state, which we refer to as *elastic* $\mu \rightarrow e$ conversion, limits the set of CLFV operators which can be probed due to the approximate parity and time-reversal symmetries of the nuclear ground state.

As the nature of potentially observable CLFV is yet unknown, one would like to consider the most general description of the $\mu \rightarrow e$ conversion process in the form of an effective theory with unknown parameters, or low-energy constants (LECs), that can be constrained by experiment. Recently, an effective theory description of elastic $\mu \rightarrow e$ conversion was formulated in terms of non-relativistic single-nucleon currents interacting with the leptons [1, 2]. This effective theory factorizes the CLFV physics – which is independent of the target nucleus – from the nuclear physics, allowing one to directly access the “nuclear dials” which can be tuned through clever target selection to extract all of the information about the underlying CLFV physics that is available in the low-energy, highly-exclusive process of elastic $\mu \rightarrow e$ conversion. Here, we summarize the recent development of the nucleon-level effective theory of $\mu \rightarrow e$ conversion including the approximations necessary to achieve a simple, factorized expression for the CLFV decay rate.

2. Treatment of lepton wave functions

Highly-accurate numerical wave functions for the bound muon and outgoing electron can be obtained by solving the Dirac equation in the nuclear Coulomb field. The effect of the finite nuclear size is accounted for by considering a nuclear charge density $\rho_p(r)$ that has been fit to electron

scattering data [7]. Many previous studies (e.g. [8–12]) of $\mu \rightarrow e$ conversion have restricted attention to the case of coherent conversion in which the relevant nuclear operators sum coherently over all A nucleons in the nucleus leading to a naive enhancement of A relative to non-coherent operators. The simple form of the coherent operators implies that their nuclear matrix elements depend only on the isoscalar nuclear density, a measured quantity. In the coherent case, it is therefore justified to use the highly-accurate numerical lepton wave functions. This leads to a “top-down” approach in which a candidate CLFV model (or class of models) is considered which generates at leading order a coherent response. The $\mu \rightarrow e$ branching ratio can be computed with quantified uncertainties and therefore used to exclude regions of parameter space within the models under consideration.

On the other hand, to pursue the “bottom-up” approach of considering the most general theory of $\mu \rightarrow e$ conversion is cumbersome if one wants to retain the numerical lepton wave functions and requires the calculation of nuclear response functions which typically do not have well understood uncertainties. In order to achieve a relatively simple theory which factorizes the CLFV physics from the nuclear physics we introduce approximate forms for the muon and electron wave functions.

The captured muon quickly decays to the $1s$ orbital of the nuclear Coulomb field. For the light nuclei ($\alpha Z \ll 1$) that we consider here, the bound muon is highly non-relativistic, and we neglect entirely the lower component of the wave function. In the nucleus ^{27}Al , the muonic Bohr radius $a_\mu^0 \approx 19.7$ fm is large compared to both the nuclear size $r_N^{\text{rms}} \approx 3.1$ fm and the scale over which the electron wave function varies, which is given by the first zero of the Bessel function $j_0(qr)$, $r_e \approx \frac{\pi}{q} \approx \frac{\pi}{m_\mu} \approx 5.9$ fm. Therefore it is a suitable approximation to replace the complicated numerical solution by a constant value. In the limit of a point-like nucleus, the appropriate constant would be the value of the muon wave function evaluated at the origin. Furthermore, for a point-like nucleus the Schrodinger solution for the muon wave function reduces to a known analytic form which, evaluated at the origin yields

$$\phi_{1s}^Z(\vec{r} = 0) = \frac{1}{\sqrt{4\pi}} \left[\frac{Z\alpha\mu c}{\hbar} \right]^{3/2}, \quad (2)$$

where μ is the muon reduced mass. With this limit in mind, we choose to parameterize the constant approximation for the muon wave function in terms of an effective point-like nuclear charge Z_{eff} seen by the muon

$$\phi_{1s}^{Z_{\text{eff}}}(\vec{r} = 0) = \frac{1}{\sqrt{4\pi}} \left[\frac{Z_{\text{eff}}\alpha\mu c}{\hbar} \right]^{3/2} \equiv \frac{1}{\sqrt{4\pi}} \frac{\int dr r^2 \rho_N(r) j_0(qr) \frac{G(r)}{r}}{\int dr r^2 \rho_N(r) j_0(qr)}, \quad (3)$$

where $\rho_N(r)$ is the nuclear density and $G(r)$ is the upper component of the muon’s radial Dirac wave function. We find $Z_{\text{eff}} = 11.309$ and 16.656 for Al and Ti, respectively. Fig. 1 compares the constant approximation of the muon wave function in the target nuclei ^{27}Al and ^{48}Ti to the Dirac solutions obtained from the extended nuclear charge densities. The constant approximation is chosen to exactly reproduce the isoscalar monopole operator which contributes to coherent $\mu \rightarrow e$ conversion but will introduce some error when used to compute matrix elements of different multipole operators as the radial weighting will differ from the monopole density. We estimate that the muon approximations induce an overall error in the decay rate $\sim 1\%$ in Al and $\sim 4\%$ in Ti,

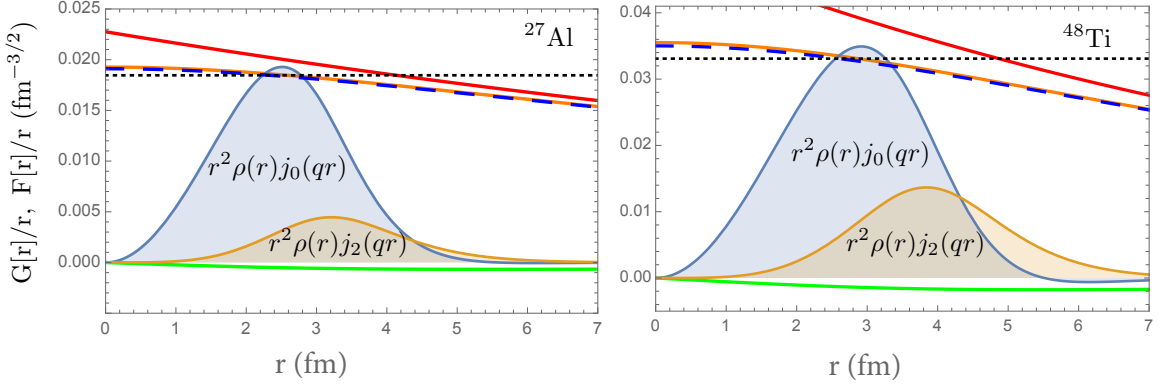


Figure 1: Muon $1s$ bound state wave functions for ^{27}Al (left) and ^{48}Ti (right) including the Dirac $\kappa = -1$ upper $G(r)$ (orange) and lower $F(r)$ (green), and Schrodinger (blue dashed) solutions for the extended nuclear charge distribution, and the Schrodinger solution of a point-like nuclear charge (red); also shown are the volume-weighted charge distributions $r^2\rho(r)j_0(qr)$ and $r^2\rho(r)j_2(qr)$ (shaded). The overall normalization (but not the relative normalization) of the two densities is arbitrary. As the muon wave function varies slowly over the nucleus, it is appropriate to use an average value: the black dotted line is the constant approximation obtained via Eq. 3.

which is typically less than the uncertainty associated with the evaluation of the nuclear response functions.

The outgoing electron receives nearly all of the muon rest mass energy as kinetic energy and is therefore ultra-relativistic. Although nearly a Dirac plane wave, the electron wave function is distorted by the Coulomb interaction with the nuclear charge. The effect of Coulomb attraction can be accounted for while retaining a simple plane wave form by introducing an effective momentum q_{eff} [13, 14] for the electron so that its wave function can be written as

$$U(q, s) e^{i\vec{q}\cdot\vec{x}} \rightarrow \sqrt{\frac{E_e}{2m_e}} \begin{pmatrix} \xi_x \\ \vec{\sigma} \cdot \hat{q} \xi_s \end{pmatrix} \frac{q_{\text{eff}}}{q} e^{i\vec{q}_{\text{eff}}\cdot\vec{x}}. \quad (4)$$

The effective momentum q_{eff} is equated to the physical momentum minus the (negative) average Coulomb potential energy over the nuclear charge density. In particular, we find $q_{\text{eff}} = 110.81$ MeV and 112.43 MeV for ^{27}Al and ^{48}Ti , respectively. The resulting effective momentum approximation for the electron wave function in various partial waves for the nucleus ^{27}Al is shown in Fig. 2. The quality of the effective momentum approximation for Ti is similar to that of Al.

3. Nucleon-level effective theory

When the approximate lepton wave functions are coupled to non-relativistic single-nucleon currents, the resulting theory may be expressed entirely in terms of operators acting between Pauli spinors. All of the operators in the theory can then be constructed from the identity operators for the leptons and nucleons – respectively, 1_L and 1_N – and the following four Hermitian vector operators:

$$i\hat{q} = \frac{i\vec{q}}{|\vec{q}|}, \vec{v}_N, \vec{\sigma}_L, \vec{\sigma}_N, \quad (5)$$

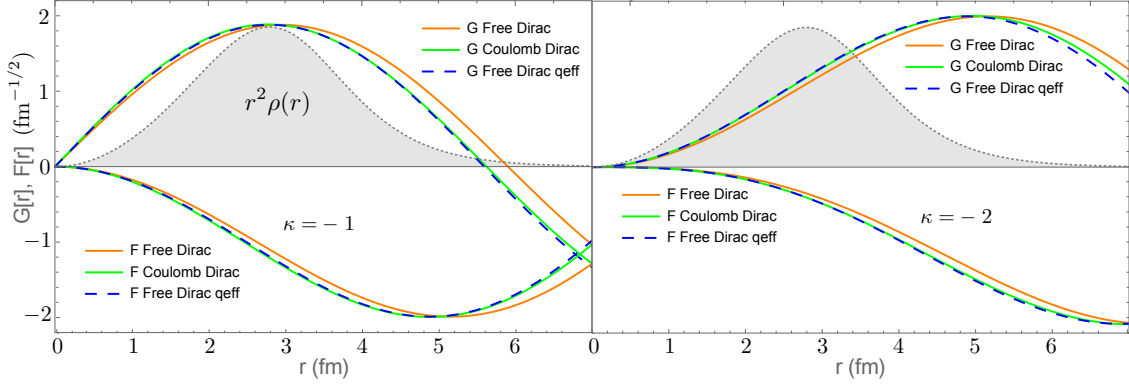


Figure 2: The Dirac Coulomb solutions $G(r)$ and $F(r)$ for the highly relativistic outgoing electron produced in $\mu \rightarrow e$ conversion in ^{27}Al (green line) are compared to the free solution (orange) and to the free solution evaluated with \vec{q}_{eff} (blue dashed), for low partial waves ($\kappa = -1, -2$). The nuclear charge distribution is shown by the shading (arbitrary normalization). The agreement between the Coulomb and plane wave solutions evaluated with q_{eff} is quite good, particularly over the relevant region where the nuclear density is concentrated.

where \hat{q} is the direction of the outgoing electron and $\vec{v}_N = (\vec{p}_i + \vec{p}_f)/(2m_N)$ is the average nucleon velocity. Working to first order in v_N , we identify 16 independent scalar operators that can be formed from the six building block operators

$$\begin{aligned}
 O_1 &= 1_L 1_N & O'_2 &= 1_L i\hat{q} \cdot \vec{v}_N & O_3 &= 1_L i\hat{q} \cdot [\vec{v}_N \times \vec{\sigma}_N] \\
 O_4 &= \vec{\sigma}_L \cdot \vec{\sigma}_N & O_5 &= \vec{\sigma}_L \cdot (i\hat{q} \times \vec{v}_N) & O_6 &= i\hat{q} \cdot \vec{\sigma}_L i\hat{q} \cdot \vec{\sigma}_N \\
 O_7 &= 1_L \vec{v}_N \cdot \vec{\sigma}_N & O_8 &= \vec{\sigma}_L \cdot \vec{v}_N & O_9 &= \vec{\sigma}_L \cdot (i\hat{q} \times \vec{\sigma}_N) \\
 O_{10} &= 1_L i\hat{q} \cdot \vec{\sigma}_N & O_{11} &= i\hat{q} \cdot \vec{\sigma}_L 1_N & O_{12} &= \vec{\sigma}_L \cdot [\vec{v} \times \vec{\sigma}_N] \\
 O'_{13} &= \vec{\sigma}_L \cdot (i\hat{q} \times [\vec{v}_N \times \vec{\sigma}_N]) & O_{14} &= i\hat{q} \cdot \vec{\sigma}_L \vec{v}_N \cdot \vec{\sigma}_N & O_{15} &= i\hat{q} \cdot \vec{\sigma}_L i\hat{q} \cdot [\vec{v}_N \times \vec{\sigma}_N] \\
 O'_{16} &= i\hat{q} \cdot \vec{\sigma}_L i\hat{q} \cdot \vec{v}_N
 \end{aligned} \tag{6}$$

Normalized to the scale of the weak interaction, the effective Lagrangian can be expressed in terms of dimensionless LECs \tilde{c}_i^τ as

$$\mathcal{L}_{\text{eff}} = \sqrt{2}G_F \sum_{\tau=0,1} \sum_{i=1}^{16} \tilde{c}_i^\tau O_i t^\tau, \tag{7}$$

where G_F is the Fermi constant and, allowing for different couplings to protons and neutrons, we have introduced isoscalar $t^0 = 1$ and isovector $t^1 = \tau_3$ operators.

Constructed in terms of contact interactions between leptonic and one-body nuclear currents, the nucleon-level ET does not explicitly include pions or other mesons, hadronic resonances, or two-body and higher nuclear currents. In the absence of these additional degrees of freedom, the \tilde{c}_i s are independent of the target nucleus in which the theory is embedded. On the other hand, including for example pion exchange will introduce form factors $f(q/m_\pi)$ which depend on the nuclear target through the momentum-transfer. As the form factors are evaluated at fixed three-momentum transfer q and the magnitude of the three-momentum transfer does not depend strongly on the nuclear target – q varies from 104.98 MeV for Al to 104.28 MeV for Ti – we expect that one may absorb the form factor into the corresponding LECs while introducing only a marginal target-dependence.

Similarly, the single-nucleon effective theory is still valid when higher-body nuclear interactions contribute. It has been demonstrated that the next-to-leading order (NLO) two-nucleon contribution to scalar-mediated coherent $\mu \rightarrow e$ conversion can be described by an effective single-nucleon operator, obtained by averaging the two-nucleon operator over a degenerate Fermi gas model of the target nucleus [10, 15]. We expect that a generic two-nucleon operator can be reduced to an effective single-nucleon operator as

$$\mathcal{O}^{(2)} \rightarrow \sum_{\tau=0,1} \sum_{i=1}^{16} f_i^\tau \mathcal{O}_i t^\tau, \quad (8)$$

where the effective couplings f_i^τ depend on the nuclear density of the target. In direct analogy with the treatment of propagator effects, the impact of two-nucleon operators can thus be absorbed into the LECs of the single-nucleon effective theory, introducing a dependence of the LECs on the nuclear target which we anticipate will be weak as long as the higher-body terms enter at higher orders.

The LECs of the nucleon-level effective theory can be matched to the LECs of effective theories at higher energy scales such as chiral perturbation theory, which can in turn be matched to standard model effective theories involving quark degrees of freedom. In this way, constraints obtained on the c_i^τ s can be translated into constraints on the parameters in candidate UV theories of CLFV. Given the close correspondence between the nucleon-level effective theory of $\mu \rightarrow e$ conversion and nucleon-level effective theories of WIMP dark matter scattering with nuclei [16, 17], many of the required matching relationships have already been derived [18–23].

4. Expression for the decay rate

The 16 CLFV operators that form the basis of the nucleon-level effective theory contain two nuclear charges, 1_N and $\vec{v}_N \cdot \vec{\sigma}_N$, and three nuclear currents, \vec{v}_N , $\vec{\sigma}_N$ and $\vec{v}_N \times \vec{\sigma}_N$, which upon multipole projection with respect to the momentum transfer \hat{q} give rise to 11 independent single-nucleon response functions shown in Table 1. Of the eleven single-nucleon response operators, only six possess multipoles which are simultaneously even under both parity and time-reversal and therefore contribute to elastic $\mu \rightarrow e$ conversion. The notation M_J , $\tilde{\Omega}_J$, etc. is standard in the study of semi-leptonic weak interactions, and complete expressions may be found, for example, in [17, 24].

The CLFV $\mu \rightarrow e$ decay rate can then be expressed as

$$\begin{aligned} \omega = \frac{G_F^2}{\pi} \frac{q_{\text{eff}}^2}{1 + \frac{q}{M_T}} |\phi_{1s}^{Z_{\text{eff}}}(\vec{0})|^2 \sum_{\tau=0,1} \sum_{\tau'=0,1} \left\{ \left[\tilde{R}_M^{\tau\tau'} W_M^{\tau\tau'}(q_{\text{eff}}) + \tilde{R}_{\Sigma''}^{\tau\tau'} W_{\Sigma''}^{\tau\tau'}(q_{\text{eff}}) + \tilde{R}_{\Sigma'}^{\tau\tau'} W_{\Sigma'}^{\tau\tau'}(q_{\text{eff}}) \right] \right. \\ \left. + \frac{q_{\text{eff}}^2}{m_N^2} \left[\tilde{R}_{\Phi''}^{\tau\tau'} W_{\Phi''}^{\tau\tau'}(q_{\text{eff}}) + \tilde{R}_{\Phi'}^{\tau\tau'} W_{\Phi'}^{\tau\tau'}(q_{\text{eff}}) + \tilde{R}_{\Delta}^{\tau\tau'} W_{\Delta}^{\tau\tau'}(q_{\text{eff}}) \right] \right. \\ \left. - \frac{2q_{\text{eff}}}{m_N} \left[\tilde{R}_{\Phi''M}^{\tau\tau'} W_{\Phi''M}^{\tau\tau'}(q_{\text{eff}}) + \tilde{R}_{\Delta\Sigma'}^{\tau\tau'} W_{\Delta\Sigma'}^{\tau\tau'}(q_{\text{eff}}) \right] \right\} \quad (9) \end{aligned}$$

Charge/Current	Projection	Operator	Even J	Odd J	LECs Probed
1_N	Charge	M_{JM}	E-E	O-O	c_1, c_{11}
$\vec{v}_N \cdot \vec{\sigma}_N$	Charge	$\tilde{\Omega}_{JM}$	O-E	E-O	c_7, c_{14}
\vec{v}_N	Longitudinal	$\tilde{\Delta}'_{JM}$	E-O	O-E	c_2, c_8, c_{16}
"	Transverse magnetic	Δ_{JM}	O-O	E-E	c_5, c_8
"	Transverse electric	Δ'_{JM}	E-O	O-E	c_5, c_8
$\vec{\sigma}_N$	Longitudinal	Σ''_{JM}	O-O	E-E	c_4, c_6, c_{10}
"	Transverse magnetic	Σ_{JM}	E-O	O-E	c_4, c_9
"	Transverse electric	Σ'_{JM}	O-O	E-E	c_4, c_9
$\vec{v}_N \times \vec{\sigma}_N$	Longitudinal	Φ''_{JM}	E-E	O-O	c_3, c_{12}, c_{15}
"	Transverse magnetic	$\tilde{\Phi}_{JM}$	O-E	E-O	c_{12}, c_{13}
"	Transverse electric	$\tilde{\Phi}'_{JM}$	E-E	O-O	c_{12}, c_{13}

Table 1: The eleven single-nucleon response functions, the charges/currents and multipole projections from which they arise, their transformation properties under parity and time-reversal for even J and odd J , and the LECs of the effective theory which they probe. Highlighted in blue are the multipole operators which contribute to elastic $\mu \rightarrow e$ conversion.

where M_T is the mass of the target nucleus and the decay rate has been factorized into a sum of products of dimensionless CLFV response functions

$$\begin{aligned}
 \tilde{R}_M^{\tau\tau'} &= \tilde{c}_1^\tau \tilde{c}_1^{\tau'*} + \tilde{c}_{11}^\tau \tilde{c}_{11}^{\tau'*} & \tilde{R}_{\Sigma''}^{\tau\tau'} &= (\tilde{c}_4^\tau - \tilde{c}_6^\tau)(\tilde{c}_4^{\tau'*} - \tilde{c}_6^{\tau'*}) + \tilde{c}_{10}^\tau \tilde{c}_{10}^{\tau'*} \\
 \tilde{R}_{\Sigma'}^{\tau\tau'} &= \tilde{c}_4^\tau \tilde{c}_4^{\tau'*} + \tilde{c}_9^\tau \tilde{c}_9^{\tau'*} & \tilde{R}_{\Phi''}^{\tau\tau'} &= \tilde{c}_3^\tau \tilde{c}_3^{\tau'*} + (\tilde{c}_{12}^\tau - \tilde{c}_{15}^\tau)(\tilde{c}_{12}^{\tau'*} - \tilde{c}_{15}^{\tau'*}) \\
 \tilde{R}_{\Phi'}^{\tau\tau'} &= \tilde{c}_{12}^\tau \tilde{c}_{12}^{\tau'*} + \tilde{c}_{13}^\tau \tilde{c}_{13}^{\tau'*} & \tilde{R}_{\Delta}^{\tau\tau'} &= \tilde{c}_5^\tau \tilde{c}_5^{\tau'*} + \tilde{c}_8^\tau \tilde{c}_8^{\tau'*} \\
 \tilde{R}_{\Phi''M}^{\tau\tau'} &= \text{Re} [\tilde{c}_3^\tau \tilde{c}_1^{\tau'*} - (\tilde{c}_{12}^\tau - \tilde{c}_{15}^\tau) \tilde{c}_{11}^{\tau'*}] & \tilde{R}_{\Delta\Sigma'}^{\tau\tau'} &= \text{Re} [\tilde{c}_5^\tau \tilde{c}_4^{\tau'*} + \tilde{c}_8^\tau \tilde{c}_9^{\tau'*}],
 \end{aligned} \tag{10}$$

and dimensionless nuclear response functions $W_O^{\tau\tau'}(q_{\text{eff}})$. In addition to the six independent nuclear responses, we find two interference terms arising, respectively, from the mixing of charge (M_J) with longitudinal (Φ''_J) multipoles, and transverse electric (Σ''_J) with transverse-magnetic (Δ_J) multipoles.

The factorized form of the effective theory dictates how much information about CLFV operators is probed in elastic $\mu \rightarrow e$ conversion experiments. Specifically, by varying the nuclear target one can hope to constrain the values of the CLFV response functions $\tilde{R}_O^{\tau\tau'}$; it is not possible, however, to parse out the values of the LECs of individual CLFV operators \tilde{c}_i^τ . Of the 16 LECs in the effective theory four of them $\tilde{c}_2, \tilde{c}_7, \tilde{c}_{14}$ and \tilde{c}_{16} do not appear in Eq. 10 and therefore are not probed in elastic $\mu \rightarrow e$ conversion due to the parity and time-reversal constraints imposed by the nuclear ground state. These operators can contribute if one considers the case where the nucleus is allowed to transition to an excited state.

5. Limits on LECs

To make contact with experiments, the decay rate obtained in Eq. 9 is converted to a branching ratio by normalizing by the rate of standard muon capture in the target nucleus [25]. For a given

Coupling	Target (Branching Ratio)			
	Al (10^{-17})		Ti (6.1×10^{-13} [26])	
	$\tau = 0$	$\tau = 1$	$\tau = 0$	$\tau = 1$
$\tilde{c}_1, \tilde{c}_{11}$	10,000 TeV	2,000 TeV	900 TeV	200 TeV
$\tilde{c}_3, \tilde{c}_{15}$	2,000 TeV	600 TeV	100 TeV	90 TeV
\tilde{c}_4	2,000 TeV	2,000 TeV	60 TeV	60 TeV
\tilde{c}_5, \tilde{c}_8	900 TeV	700 TeV	30 TeV	30 TeV
$\tilde{c}_6, \tilde{c}_{10}$	2,000 TeV	2,000 TeV	60 TeV	60 TeV
\tilde{c}_9	2,000 TeV	1,000 TeV	50 TeV	40 TeV
\tilde{c}_{12}	2,000 TeV	700 TeV	100 TeV	90 TeV
\tilde{c}_{13}	200 TeV	500 TeV	30 TeV	10 TeV

Table 2: Approximate scale Λ_i^τ of new physics probed by each LEC for a given nuclear target and branching ratio limit.

target, the lepton approximation parameters q_{eff} and Z_{eff} are computed, and the nuclear response functions $W_O(q_{\text{eff}})$ are evaluated, for example, using the nuclear shell model, allowing us to express the branching ratio in terms of the only unknown parameters, the \tilde{c}_i s. We may then assess the sensitivity of the branching ratio to each operator in the theory by turning on a single LEC at a time and determining the largest value of the LEC consistent with the known branching ratio limit; that is, we can determine y_i^τ such that $|\tilde{c}_i^\tau| \leq y_i^\tau$ in order that the branching ratio not exceed the specified limit. More physically, if we assume that the dimensionless LEC under consideration is natural at the scale associated with CLFV physics, we can translate the limit y_i^τ into an approximate scale probed by the given operator

$$\Lambda_i^\tau \sim \left(\frac{1}{\sqrt{2}G_F y_i^\tau} \right)^{1/2} \quad (11)$$

Table 2 shows the approximate scale Λ_i^τ probed by each LEC for an existing branching ratio limit in Ti and for the branching ratio limit goal of the Mu2e and COMET experiments in Al. To evaluate the nuclear response functions, we performed nuclear shell model calculations using the configuration-interaction code BIGSTICK [27, 28] and the USDB $2s1d$ [29] and KB3G $2p1f$ [30] interactions for Al and Ti, respectively. Harmonic oscillator parameters $b = 1.84$ fm for Al and $b = 1.99$ fm for Ti were employed. Further details of the nucleon-level effective theory as well as calculations for additional target nuclei may be found in [2].

Acknowledgments

I would like to acknowledge and thank my collaborators on the nucleon-level effective theory of $\mu \rightarrow e$ conversion: Wick C. Haxton, Kenneth McElvain, and Michael J. Ramsey-Musolf. This work was supported in part by the U.S. Department of Energy under grants DE-SC0004658, DE-FOA-0001269 and FWP-NQISCAWL.

References

- [1] E. Rule, W.C. Haxton and K. McElvain, *Nucleon-level effective theory of $\mu \rightarrow e$ conversion*, [2109.13503](#).
- [2] W.C. Haxton, E. Rule, K. McElvain and M.J. Ramsey-Musolf, *Nucleon-level effective theory of $\mu \rightarrow e$ conversion in the nuclear field*, *In Preparation* (2022) .
- [3] SINDRUM II collaboration, *A Search for muon to electron conversion in muonic gold*, *Eur. Phys. J. C* **47** (2006) 337.
- [4] Mu2E collaboration, *Mu2e Technical Design Report*, [1501.05241](#).
- [5] Mu2E collaboration, *Expression of Interest for Evolution of the Mu2e Experiment*, [1802.02599](#).
- [6] COMET collaboration, *COMET Phase-I Technical Design Report*, *PTEP* **2020** (2020) 033C01 [[1812.09018](#)].
- [7] H. De Vries, C. De Jager and C. De Vries, *Nuclear charge-density-distribution parameters from elastic electron scattering*, *Atomic Data and Nuclear Data Tables* **36** (1987) 495.
- [8] A. Czarnecki, W.J. Marciano and K. Melnikov, *Coherent muon-electron conversion in muonic atoms*, *The workshop on physics at the first muon collider and at the front end of a muon collider* (1998) .
- [9] R. Kitano, M. Koike and Y. Okada, *Detailed calculation of lepton flavor violating muon electron conversion rate for various nuclei*, *Phys. Rev. D* **66** (2002) 096002 [[hep-ph/0203110](#)].
- [10] A. Bartolotta and M.J. Ramsey-Musolf, *Coherent μ -e conversion at next-to-leading order*, *Phys. Rev. C* **98** (2018) 015208 [[1710.02129](#)].
- [11] A. Crivellin, M. Hoferichter and M. Procura, *Improved predictions for $\mu \rightarrow e$ conversion in nuclei and higgs-induced lepton flavor violation*, *Phys. Rev. D* **89** (2014) 093024.
- [12] V. Cirigliano, R. Kitano, Y. Okada and P. Tuzon, *On the model discriminating power of $\mu \rightarrow e$ conversion in nuclei*, *Phys. Rev. D* **80** (2009) 013002 [[0904.0957](#)].
- [13] J. Knoll, *An analytic description of inelastic electron scattering on nuclei*, *Nuclear Physics A* **223** (1974) 462.
- [14] F. Lenz and R. Rosenfelder, *Nuclear radii in the high-energy limit of elastic electron scattering*, *Nuclear Physics A* **176** (1971) 513.
- [15] V. Cirigliano, K. Fuyuto, M.J. Ramsey-Musolf and E. Rule, *Next-to-leading order scalar contributions to $\mu \rightarrow e$ conversion*, *In Preparation* (2022) .

- [16] A.L. Fitzpatrick, W. Haxton, E. Katz, N. Lubbers and Y. Xu, *The effective field theory of dark matter direct detection*, *Journal of Cosmology and Astroparticle Physics* **2013** (2013) 004–004.
- [17] N. Anand, A.L. Fitzpatrick and W.C. Haxton, *Weakly interacting massive particle-nucleus elastic scattering response*, *Phys. Rev. C* **89** (2014) 065501.
- [18] J. Fan, M. Reece and L.-T. Wang, *Non-relativistic effective theory of dark matter direct detection*, *Journal of Cosmology and Astroparticle Physics* **2010** (2010) 042–042.
- [19] F. Bishara, J. Brod, B. Grinstein and J. Zupan, *Chiral effective theory of dark matter direct detection*, *Journal of Cosmology and Astroparticle Physics* **2017** (2017) 009–009.
- [20] J. Brod, A. Gootjes-Dreesbach, M. Tamaro and J. Zupan, *Effective field theory for dark matter direct detection up to dimension seven*, *Journal of High Energy Physics* **2018** (2018) .
- [21] M. Cirelli, E.D. Nobile and P. Panci, *Tools for model-independent bounds in direct dark matter searches*, *Journal of Cosmology and Astroparticle Physics* **2013** (2013) 019–019.
- [22] G. Barello, S. Chang and C.A. Newby, *A model independent approach to inelastic dark matter scattering*, *Phys. Rev. D* **90** (2014) 094027.
- [23] R.J. Hill and M.P. Solon, *Standard model anatomy of wimp dark matter direct detection. ii. qcd analysis and hadronic matrix elements*, *Phys. Rev. D* **91** (2015) 043505.
- [24] T. Donnelly and W. Haxton, *Multipole operators in semileptonic weak and electromagnetic interactions with nuclei: Harmonic oscillator single-particle matrix elements*, *Atomic Data and Nuclear Data Tables* **23** (1979) 103 .
- [25] T. Suzuki, D.F. Measday and J.P. Roalsvig, *Total nuclear capture rates for negative muons*, *Phys. Rev. C* **35** (1987) 2212.
- [26] P. Wintz in *Proc. 1st Int. Symp. on Lepton and Baryon Number Violation*, H.V. Klapdor-Kleingrothaus and I.V. Krivosheina, eds., p. 534, IOP Publishing, 1999.
- [27] C.W. Johnson, W.E. Ormand and P.G. Krastev, *Factorization in large-scale many-body calculations*, *Computer Physics Communications* **184** (2013) 2761 [1303.0905].
- [28] C.W. Johnson, W.E. Ormand, K.S. McElvain and H. Shan, *BIGSTICK: A flexible configuration-interaction shell-model code*, *arXiv e-prints* (2018) arXiv:1801.08432 [1801.08432].
- [29] B.A. Brown and W.A. Richter, *New “usd” hamiltonians for the sd shell*, *Phys. Rev. C* **74** (2006) 034315.
- [30] A. Poves, J. Sánchez-Solano, E. Caurier and F. Nowacki, *Shell model study of the isobaric chains $a=50$, $a=51$ and $a=52$* , *Nuclear Physics A* **694** (2001) 157–198.